VII International Conference on Computational Methods for Coupled Problems in Science and Engineering
COUPLED PROBLEMS 2017
M. Papadrakakis, E. Oñate and B. Schrefler (Eds)

CONJUGATE HEAT TRANSFER SHAPE OPTIMIZATION BASED ON THE CONTINUOUS ADJOINT METHOD

K.T. GKARAGKOUNIS*, E.M. PAPOUTSIS-KIACHAGIAS† AND K.C. GIANNAKOGLOU††

Lab. of Thermal Turbomachines, Parallel CFD & Optimization Unit
National Technical University of Athens
9, Heroon Polytechniou, NTUA Zografou Campus, 15780, Athens, Greece
e-mails: kogkar@hotmail.com*, vaggelisp@gmail.com† and kgianna@central.ntua.gr††
††web page: http://velos0.ltt.mech.ntua.gr/research/

Key words: Continuous Adjoint Method, Conjugate Heat Transfer, Shape Optimization, Fluid-Solid Interface.

Summary: In this paper, the continuous adjoint method for use in gradient-based optimization methods for coupled problems including heat transfer between bodies (solids) and fluids flowing over or inside them is developed. This kind of problems are usually referred to as Conjugate Heat Transfer (CHT) problems. Emphasis is given to expanding the Enhanced-Surface Integral (E-SI) adjoint formulation recently published by the authors' group for shape optimization problems in fluid mechanics only, to tackle CHT problems. This formulation ensures that the gradient of the objective function is accurately computed, while the computational cost is kept as low as possible.

1 INTRODUCTION

Adjoint methods have widely been used to solve single-discipline optimization problems. However, the advances in computational methods and the capabilities of modern computational platforms have shifted the interest from single-discipline to coupled problems [2]. CHT problems, involving the interaction of fluid flow and heat transfer between fluids and solids, are investigated in this paper, by focusing on the development of the continuous adjoint method for use in the optimization of the shape of solid boundaries/interfaces. To the authors' knowledge, there are a few papers in the literature of continuous adjoint methods which are related to CHT shape optimization problems [3, 9].

The first goal of this paper is to expand a new continuous adjoint formulation, the so-called E-SI one, to CHT problems. This formulation, initially proposed by the authors' group in [7], was originally developed for shape optimization problems in incompressible fluid flows. More convincing applications of the same method, for other objective functions, can be found in [8].

The second goal of this paper is to compare the E-SI formulation as developed for CHT problems with alternative formulations of the continuous adjoint method, according to the literature. As presented in [7, 8], there are two other continuous adjoint formulations, yielding different sensitivity derivative (SD) expressions. The first one is referred to as FI (Field Integral), since the resulting SD expression includes at least one field integral over the solution domain. This method computes accurate SD with computational cost though, that scales with the number of the design (or optimization) variables parameterizing the shape to be designed [4]. The second formulation [1, 5, 10] leads to exactly the same adjoint PDEs and boundary conditions, though to different expressions for the SD, which are now exclusively expressed in terms of surface integrals; this is referred to as the SI (Surface Integral) adjoint formulation. SD computed using the SI adjoint might generally become quite inaccurate; however, the SI formulation is appealing due to its low cost which does not depend on the number of design variables.

In the E-SI adjoint method, apart from the flow PDEs or the heat conduction equation over the solid domain, also the adjoint to the grid displacement equations must be solved. This method computes SD expressed in terms of surface integrals, enhanced with the contributions from the adjoint to the grid displacement PDEs.

The mathematical development includes the formulation of the adjoint to the Fluid-Structure Interface (FSI) conditions. The three continuous adjoint formulations are investigated through applications in 2D problems and the accuracy of the computed SD is validated by comparing them with finite differences (FD).

2 PRIMAL PROBLEM

The overall computational domain Ω comprises the fluid Ω_F and solid Ω_S subdomains, separated by an interface $\overline{S}$. Depending on whether the interface is seen from the fluid or solid point of view, the latter will be denoted by $\overline{S}_F$ or $\overline{S}_S$, respectively. The steady-state Navier-Stokes equations for incompressible fluid flows are given by

$$R^p = -\frac{\partial v_j}{\partial x_j} = 0 \tag{1}$$

$$R_i^v = v_j \frac{\partial v_i}{\partial x_j} - \frac{\partial \tau_{ij}}{\partial x_j} + \frac{\partial p}{\partial x_i} = 0 \tag{2}$$

$$R_F^T = v_j c_p \frac{\partial T^F}{\partial x_j} + \frac{v_j}{2}\frac{\partial v_k^2}{\partial x_j} - \frac{\partial}{\partial x_j}\left(a_{eff} c_p \frac{\partial T^F}{\partial x_j}\right) = 0 \tag{3}$$

where v_i are the velocity components and p stands for the static pressure divided by the fluid density ρ_F. Also, $\tau_{ij} = \nu_{eff}\left(\frac{\partial v_i}{\partial x_j} + \frac{\partial v_j}{\partial x_i}\right)$, where ν_{eff} is the effective viscosity, being either $\nu_{eff} = \nu$ for laminar or $\nu_{eff} = \nu + \nu_t$ for turbulent flows (ν, ν_t stand for the bulk and turbulent viscosities). The same holds for the thermal diffusivity α_{eff}, being either $\alpha_{eff} = \alpha$ or $\alpha_{eff} = \alpha + \alpha_t$ in laminar and turbulent flows respectively, where $\alpha = \nu/Pr$, $\alpha_t = \nu_t/Pr_t$ (Pr, Pr_t are the Prandtl numbers for laminar and turbulent

flows). Moreover, T^F is the fluid temperature and c_p the specific heat transfer coefficient under constant pressure. Repeated indices imply summation.

The boundaries S_F of Ω_F are decomposed as $S_F = S_{F,I} \cup S_{F,O} \cup S_{F,W} \cup \overline{S}_F$, indicating the inlet, outlet, plain and FSI solid walls, respectively. The conditions imposed on the boundaries of Ω_F are summarized in Table 1. The pressure and velocity conditions imposed along $\overline{S}_F$ and $S_{F,W}$ are identical; the temperature conditions are presented later on.

Table 1: Types of boundary conditions imposed along the boundaries of the fluid domain.

Boundary	p	v_i	T
$S_{F,I}$	zero Neumann	Dirichlet	Dirichlet
$S_{F,O}$	Dirichlet	zero Neumann	zero Neumann
$S_{F,W}$	zero Neumann	Dirichlet	zero Neumann

On the other hand, heat conduction in Ω_S is governed by

$$R_S^T = -\frac{\partial}{\partial x_j}\left[k^S \frac{\partial T^S}{\partial x_j}\right] = 0 \tag{4}$$

where k^S stands for the thermal conductivity of the solid region. The solid domain boundaries S_S are decomposed as $S_S = S_{S,o} \cup \overline{S}_S$, where $S_{S,o}$ represents boundaries other than $\overline{S}_S$. For the cases presented herein, T^S is fixed along $S_{S,o}$.

The most critical part of the CHT problem is related to the (physical) conditions imposed along each point at the FSI boundary, which are

$$k^S \frac{\partial T^S}{\partial n}\bigg|_{\overline{S}_S} = -k^F \frac{\partial T^F}{\partial n}\bigg|_{\overline{S}_F} \tag{5}$$

$$T^S = T^F \tag{6}$$

where $k^F = (a + a_t) c_p \rho_F$.

3 CONTINUOUS ADJOINT (E-SI) FORMULATION

Starting point of the continuous adjoint method, according to the E-SI formulation [7], is the augmented objective function

$$L = J + \int_{\Omega_F} q R^p d\Omega + \int_{\Omega_F} u_i R_i^v d\Omega + \sum_{D=F,S} \left\{ \int_{\Omega_D} T_a^D R_D^T d\Omega + \int_{\Omega_D} m_{a,i}^D R_{D,i}^m d\Omega \right\} \tag{7}$$

where $D = F, S$. The objective function J to be minimized, is defined over Ω_S and depends solely on T^S. Also, q, u_i, T_a^D, m_a^D are the adjoint pressure and adjoint velocity

components over Ω_F, the adjoint temperature and the adjoint nodal displacement fields for the $D = F, S$ domains. According to the E-SI adjoint formulation, as proposed in [7, 8], apart from the flow/heat equations, L should also include PDEs governing the Ω_F and Ω_S grid displacement $R^m_{D,i}$. Assuming that, in both domains D, the same Laplacian grid displacement model is valid, $R^m_{D,i}$ can be expressed as

$$R^m_{D,i} = \frac{\partial^2 m^D_i}{\partial x^2_j} = 0,\ D = F, S,\ i = 1, 2, 3 \tag{8}$$

where m^D_i is the nodal (grid) displacement field over domain D.

For the sake of simplicity, during the presentation of the mathematical development of the adjoint CHT equations, we refrain from including the turbulence model and the corresponding adjoint equations. The interested reader should refer to [6, 12].

Development is based on the Leibniz integration rule for domains with varying boundaries, which states that, for any residual R ($R = R_p,\ R_{v_i},\ R_{T_D},\ R_{m_D}$) and adjoint variables Ψ ($\Psi = q,\ u_i,\ T^D_a,\ m^D_a$),

$$\frac{\delta}{\delta b_n}\int_{\Omega_D}\Psi R d\Omega = \int_{\Omega_D}\Psi\frac{\partial R}{\partial b_n}d\Omega + \int_{S_D}\Psi R n_k\frac{\delta x_k}{\delta b_n}dS \tag{9}$$

where n_k are the components of the unit vector normal to the given surface. Eq. 9 is used to develop the integrals on the r.h.s. of eq. 7 and also, the objective function J.

The adjoint equations arise, after eliminating the terms multiplying the variations in $p,\ v_i,\ T^D$ included in the expression of $\delta L/\delta b_n$. After a lengthy development, which is omitted in the interest of space, the field adjoint equations

$$R^q = -\frac{\partial u_j}{\partial x_j} = 0 \tag{10}$$

$$R^u_i = u_j\frac{\partial v_j}{\partial x_i} - v_j\frac{\partial u_i}{\partial x_j} - \frac{\partial \tau^a_{ij}}{\partial x_j} + \frac{\partial q}{\partial x_i} + c_p T^F_a\frac{\partial T^F}{\partial x_i} + T^F_a v_k\frac{\partial v_k}{\partial x_i} - v_i v_k\frac{\partial T^F_a}{\partial x_k} = 0,\ i = 1, 2(, 3) \tag{11}$$

$$R^{T_a}_F = -v_j\frac{\partial T^F_a}{\partial x_j} - \frac{\partial}{\partial x_j}\left(\alpha_{eff}\frac{\partial T^F_a}{\partial x_j}\right) = 0 \tag{12}$$

$$\begin{aligned} R^{m_{a,k}}_F = {} & \frac{\partial^2 m^F_{a,k}}{\partial x^2_j} - \frac{\partial}{\partial x_j}\Bigg[- u_i v_j\frac{\partial v_i}{\partial x_k} - \tau^a_{ij}\frac{\partial v_i}{\partial x_k} + u_i\frac{\partial \tau_{ij}}{\partial x_k} - u_j\frac{\partial p}{\partial x_k} + q\frac{\partial v_j}{\partial x_k} - c_p T^F_a v_j\frac{\partial T}{\partial x_k} \\ & - T^F_a v_j v_i\frac{\partial v_i}{\partial x_k} - \alpha_{eff} c_p\frac{\partial T^F_a}{\partial x_j}\frac{\partial T^F}{\partial x_k} + c_p T^F_a\frac{\partial}{\partial x_k}\left(\alpha_{eff}\frac{\partial T^F}{\partial x_j}\right)\Bigg] = 0 \end{aligned} \tag{13}$$

over Ω_F and

$$R^{T_a}_S = -\frac{\partial}{\partial x_j}\left(k^S\frac{\partial T^S_a}{\partial x_j}\right) + J_S = 0 \tag{14}$$

$$R^{m_{a,k}}_S = \frac{\partial^2 m^S_{a,k}}{\partial x^2_j} - \frac{\partial}{\partial x_j}\left(k_S T^S_a\frac{\partial^2 T^S}{\partial x_j \partial x_k} - k_S\frac{\partial T^S_a}{\partial x_j}\frac{\partial T^S}{\partial x_k}\right) + J_{M,k} = 0 \tag{15}$$

over Ω_S are defined. J_S and $J_{M,k}$ are the contributions from the differentiation of the objective function to the adjoint energy and grid displacement PDEs. The three final terms in eq. 11 are the contribution of the differentiated energy equation to the adjoint momentum equations. In addition, $\tau_{ij}^a = \nu_{eff}\left(\frac{\partial u_i}{\partial x_j} + \frac{\partial u_j}{\partial x_i}\right)$ stands for the adjoint stresses. It should also be noted that, for incompressible flows, the adjoint energy equation is decoupled from the mean flow one, since the first includes the primal velocity and the adjoint temperature. In contrast to the primal system though, the solution of the adjoint energy equations has to precede the solution of the adjoint mean flow equations. Eqs. 12 and 14 are coupled through their boundary conditions along the interface.

The adjoint boundary conditions arise, after eliminating terms in surface integrals multiplying the variations of the field variables w.r.t. b_n. For example, along the inlet, the imposed adjoint boundary conditions are

$$\frac{\partial q}{\partial n} = 0,\ u_i = 0,\ T_a^F = 0,\ m_a^F = 0 \tag{16}$$

Along the other non-FSI boundaries, the boundary conditions are obtained through a development similar to that in [7]. Along the FSI boundaries, the adjoint boundary conditions are similar to the primal ones. The SD expression, including only surface integrals, becomes

$$\begin{aligned}
\left.\frac{\delta J}{\delta b_n}\right|_{E-SI} = & T^J_{surface} - \int_{S_{F,W},\overline{S}_F} \left[\tau_{ij}^a n_j - q n_i\right] \frac{\partial v_i}{\partial x_k}\frac{\delta x_k}{\delta b_n} dS + \int_{S_{F,W}} \alpha_{eff} c_p T_a^F \frac{\partial T^F}{\partial x_j}\frac{\delta n_j}{\delta b_n} dS \\
& + \int_{S_{F,W}} \alpha_{eff} c_p T_a^F \frac{\partial^2 T^F}{\partial x_j \partial x_k} n_j \frac{\delta x_k}{\delta b_n} dS - \int_{S_{S,o}} k^S \frac{\partial T_a^S}{\partial x_j} n_j \frac{\partial T^S}{\partial x_k}\frac{\delta x_k}{\delta b_n} dS \\
& + \int_{\overline{S}_F} \left[T_a^F \left(k^F \frac{\partial^2 T^F}{\partial x_j \partial x_k} - k^S \frac{\partial^2 T^S}{\partial x_j \partial x_k} \right) n_j - k^F \frac{\partial T_a^F}{\partial x_j} n_j \left(\frac{\partial T^F}{\partial x_k} - \frac{\partial T^S}{\partial x_k} \right) \right] \frac{\delta x_k}{\delta b_n} dS \\
& + \int_{\overline{S}_F} T_a^F \left(k^F \frac{\partial T^F}{\partial x_j} - k^S \frac{\partial T^S}{\partial x_j} \right) \frac{\delta n_j}{\delta b_n} dS - \sum_{D=F,S} \left\{ \int_{S_{D,W},\overline{S}_D} \frac{\partial m_{a,i}^D}{\partial x_j} n_j \frac{\delta x_i}{\delta b_n} dS \right\}
\end{aligned} \tag{17}$$

where $T^J_{surface}$ depends on the objective function.

4 Comparing the E-SI with the two alternative adjoint formulations

The E-SI formulation was developed to overcome the disadvantages of the standard formulations (FI and SI) of the continuous adjoint method. Through the E-SI adjoint, it is possible to compute SD as accurate as with the FI adjoint and with the same cost as with the SI adjoint.

The FI gradient arises by further developing the following equation

$$\frac{\delta L}{\delta b_n} = \frac{\delta J}{\delta b_n} + \int_{\Omega_F} q \frac{\delta R^p}{\delta b_n} d\Omega + \int_{\Omega_F} u_i \frac{\delta R_i^v}{\delta b_n} d\Omega + \int_{\Omega_F} T_a^F \frac{\delta R_F^T}{\delta b_n} d\Omega + \int_{\Omega_S} T_a^S \frac{\delta R_S^T}{\delta b_n} d\Omega \tag{18}$$

After a lengthy mathematical development, which is omitted here since it is similar to that presented in [7], the SD expression becomes

$$\begin{aligned}\left.\frac{\delta J}{\delta b_n}\right|_{FI} = \int_{\Omega_F}\Bigg[&- u_i v_j \frac{\partial v_i}{\partial x_k} - \tau_{ij}^a \frac{\partial v_i}{\partial x_k} + u_i \frac{\partial \tau_{ij}}{\partial x_k} - u_j \frac{\partial p}{\partial x_k} + q\frac{\partial v_j}{\partial x_k} - c_p T_a^F v_j \frac{\partial T}{\partial x_k} \\ &- T_a^F v_j v_i \frac{\partial v_i}{\partial x_k} - \alpha_{eff} c_p \frac{\partial T_a^F}{\partial x_j}\frac{\partial T^F}{\partial x_k} + c_p T_a^F \frac{\partial}{\partial x_k}\left(\alpha_{eff}\frac{\partial T^F}{\partial x_j}\right)\Bigg]\frac{\partial}{\partial x_j}\left(\frac{\delta x_k}{\delta b_n}\right)d\Omega \\ &+ \int_{\Omega_S}\Bigg[- k_S \frac{\partial T_a^S}{\partial x_j}\frac{\partial T^S}{\partial x_k} + k_S T_a^S \frac{\partial^2 T^S}{\partial x_j \partial x_k}\Bigg]\frac{\partial}{\partial x_j}\left(\frac{\delta x_k}{\delta b_n}\right)d\Omega + \int_{S_{F,W}} \alpha_{eff} c_p T_a^F \frac{\partial T^F}{\partial x_j}\frac{\delta n_j}{\delta b_n} dS \\ &+ \int_{\overline{S}_F} \alpha_{eff} c_p T_a^F \frac{\partial T^F}{\partial x_j}\frac{\delta n_j}{\delta b_n} dS + \int_{\overline{S}_F} k^S T_a^S \frac{\partial T^S}{\partial x_j}\frac{\delta n_j}{\delta b_n} dS + T^J_{volume} \end{aligned} \tag{19}$$

where T^J_{volume} comes from the differentiation of J. One should notice the presence of the spatial derivatives of the grid sensitivities $\delta x_k/\delta b_n$ for the entire fluid and solid domains. These quantities are computed through FD, by superimposing infinitesimally small pertubations $\pm\epsilon$ on each design variable b_n and adapting the computational grid. From this point of view, the cost of computing the FI–gradient of J scales with the number of b_n and consequently, the use of the FI formulation becomes quite expensive in problems with many design variables. Eq. 19 is complete, without any assumption made and as such, it computes accurate SD.

The development of the SI formulation starts by applying the Leibniz theorem (eq. 9) to eq. 7, in which the integrals concerning the grid displacement equations do not exist. The derivative of L now becomes

$$\begin{aligned}\frac{\delta L}{\delta b_n} = \frac{\delta J}{\delta b_n} &+ \int_{\Omega_F} q\frac{\partial R^p}{\partial b_n} d\Omega + \int_{\Omega_F} u_i \frac{\partial R_i^v}{\partial b_n} d\Omega + \int_{\Omega_F} T_a^F \frac{\partial R_F^T}{\partial b_n} d\Omega + \int_{\Omega_S} T_a^S \frac{\partial R_S^T}{\partial b_n} d\Omega \\ &+ \int_{S_F} \left(qR^p + u_i R_i^v + T_a^F R_F^T\right) n_k \frac{\delta x_k}{\delta b_n} dS + \int_{S_S} T_a^S R_S^T n_k \frac{\delta x_k}{\delta b_n} dS \end{aligned} \tag{20}$$

The last two surface integrals which include the residuals of the PDEs governing the physical problem are dropped out by those developing SI adjoint methods, under the assumption that they are zero on the boundary. This assumption is not valid and as shown in [7], is responsible for the potential loss of accuracy of the SD computed with the SI adjoint formulation (wrong or even wrongly signed SD). After a mathematical

development, the expression of the SD is given by

$$\left.\frac{\delta F_{aug}}{\delta b_n}\right|_{SI} = T^J_{surface} - \int_{S_{F,W},\overline{S}_F} \left[\tau^a_{ij} n_j - q n_i\right] \frac{\partial v_i}{\partial x_k} \frac{\delta x_k}{\delta b_n} dS + \int_{S_{F,W}} \alpha_{eff} c_p T^F_a \frac{\partial T^F}{\partial x_j} \frac{\delta n_j}{\delta b_n} dS$$
$$+ \int_{S_{F,W}} \alpha_{eff} c_p T^F_a \frac{\partial^2 T^F}{\partial x_j \partial x_k} n_j \frac{\delta x_k}{\delta b_n} dS - \int_{S_{S,o}} k^S \frac{\partial T^S_a}{\partial x_j} n_j \frac{\partial T^S}{\partial x_k} \frac{\delta x_k}{\delta b_n} dS$$
$$+ \int_{\overline{S}_F} \left[T^F_a \left(k^F \frac{\partial^2 T^F}{\partial x_j \partial x_k} - k^S \frac{\partial^2 T^S}{\partial x_j \partial x_k} \right) n_j - k^F \frac{\partial T^F_a}{\partial x_j} n_j \left(\frac{\partial T^F}{\partial x_k} - \frac{\partial T^S}{\partial x_k} \right) \right] \frac{\delta x_k}{\delta b_n} dS$$
$$+ \int_{\overline{S}_F} T^F_a \left(k^F \frac{\partial T^F}{\partial x_j} - k^S \frac{\partial T^S}{\partial x_j} \right) \frac{\delta n_j}{\delta b_n} dS \tag{21}$$

The above SD expression consists only of surface integrals without involving the (internal) grid sensitivities. This feature makes this formulation cheaper to evaluate than the FI one and the preferred way of developing the continuous adjoint method by the great majority of researchers.

In both the FI and SI formulations, the same adjoint equations and boundary conditions, as in the E-SI one, arise without involving the adjoint grid displacement equations; the latter is a task with almost negligible cost within each optimization cycle, since it requires the solution of just a single vectorial PDE per solution domain, irrespective of the number of design variables. Note that the adjoint nodal displacement equations can be solved at a post-processing level, after computing the SI derivatives which give just a part of the E-SI ones.

5 APPLICATIONS

The first application aims at comparing the SD computed by the three adjoint formulations (E-SI, FI and SI) using FD as the reference values. The objective function, related to the mean temperature over Ω_S, is

$$J_{T^S} = \frac{\int_{\Omega_S} T_S d\Omega}{\int_{\Omega_S} d\Omega} \tag{22}$$

An S-Bend 2D duct (fluid region Ω_F) in contact with a solid body Ω_S is used. In fig. 1a, the geometry along with the parameterized patches are displayed. In specific, the central part of the FSI boundary is parameterized with 12 NURBS control points, of which the first and last ones are kept fixed. SD are computed w.r.t. the x (first half points in the abscissa) and y (second half) coordinates of these control points.

The flow is laminar; flow conditions and data are shown in Table 2. In fig. 1b, it is shown that the E-SI formulation practically reproduces the FI and FD derivatives. In contrast, this is not the case for the SI derivatives, which substantially deviate from the FD, since at quite a few control points they have different signs, being also an order of magnitude off. In addition, the computation of SD with the E-SI formulation needed

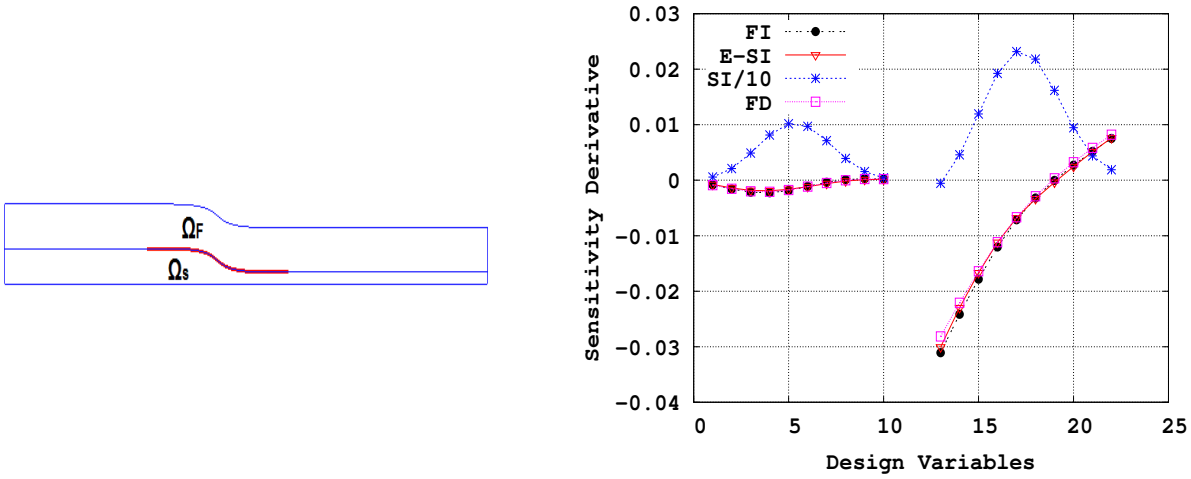

(a) (b)

Figure 1: Laminar flow in an S-Bend 2D duct ($Re = 60$), attached to a solid body. Minimization of J_{TS}. a) The fluid and solid domains along with the parameterized patch (red line). b) Comparison of SD computed with FI, E-SI, SI and FD methods.

$\sim$22 % of the time to compute them with FI, while the SI method needed $\sim$11 %. This difference in computational time between the E-SI and FI formulations increases with the number of design variables. Computations were performed in parallel on 4 Intel(R) Xeon(R) CPU E5-2630 processors at 2.30 GHz.

Table 2: Conditions and data of the two CHT problems.

S–Bend case:		**2D turbine blade case:**	
U_{inlet}	0.1 m/sec	U_{inlet}	25 m/sec
Re	60	Re	$\sim 53k$
c_p	4181 $J/kg/K$	c_p	1068 $J/kg/K$
α	1.45×10^{-6} m^2/sec	α	$\sim 93 \times 10^{-6}$ m^2/sec
Pr	6.62	Pr	0.68
k_S	60 $J/msecK$	Pr_t	1
T^F_{inlet}	291.214 K	k_S	215 $J/msecK$
T^S	300 K	T^F_{inlet}	800 K
		$T_{coolant}$	432 K
		h	2000 J/m^2secK

An optimization problem is solved in the second case. The goal is to minimize the maximum temperature of a 2D blade of a turbine stator. By definition, this is a non-differentiable function and in order to develop the continuous adjoint method for it, the

objective function used is

$$J_{maxT} = \frac{\int_{\Omega_S} \left[1 - \frac{1}{1+e^{k_2(T-T_{crit})+k_1}}\right] d\Omega}{\int_{\Omega_S} d\Omega} \tag{23}$$

where $k_1 = log\left(\frac{1}{1-f_{max}} - 1\right)$, $k_2 = \frac{log\left(\frac{1}{1-f_{max}}-1\right)}{T_{safe}-T_{crit}}$ with $f_{max} = 0.999$ and $f_{min} = 0.001$. In addition, T_{safe} and T_{crit} correspond to two different temperature limits, which are important for the operation of the blade: T_{safe} stands for the temperature below which the turbine blade is supposed to operate safely and T_{crit} for the maximum temperature which the turbine blade withstands. Here, $T_{safe} = 505\ K$ and $T_{crit} = 515\ K$.

In this problem, the flow is turbulent (the Spalart-Allmaras turbulence model [11] was used) and the blade is cooled through coolant fluid which flows through the cooling channels shown in fig. 2. Heat transfer between the coolant flowing through the cooling channels (perpendicular to the 2D mesh) and the blade body is modeled by a 1D heat transfer equation along the holes surface, which reads (h is the heat transfer coefficient)

$$k^S \frac{\partial T^S}{\partial n}\bigg|_{holes} = h\left(T_{coolant} - T^S\right) \tag{24}$$

which is imposed as a boundary condition on the holes surface. The parameterization is made with 62 NURBS control points and the SD are computed with the E-SI continuous adjoint formulation. Flow conditions and data are summarized in Table 2. After only three optimization cycles, the objective function has dropped by 9.1 %. The initial and optimal geometry are presented in figs. 2a and 2b respectively, along with T^S fields. The pressure and suction sides have come closer to the cooling holes, in order for them to lower their temperatures. In addition, the temperature distribution over Ω_S changes, as temperature values between T_{crit} and T_{safe} are observed slightly closer to the TE in the optimized geometry (figs. 2c, 2d). In the optimal geometry, the maximum temperature of the blade has dropped by 2 K (figs. 2a, 2b). In figs. 3a–3f, the primal and adjoint fields over the initial geometry are included. Finally, one should notice that the part of Ω_S with the higher (in magnitude) T_S^a is mostly changed during the optimization procedure.

6 CONCLUSIONS

The continuous adjoint method to support gradient-based optimization in conjugate heat transfer problems between fluid and solid domains has been presented, programmed in OpenFOAM and demonstrated for two objective functions. In the presented test cases, the optimization algorithm controls the shape of (part of) the interface between the fluid and solid domains. The developed continuous adjoint method(s), which can easily be extended to other objective functions, have the advantages of computing accurate gradients while being as fast as possible. To achieve this, the grid displacement equations (i.e. the PDEs which undertake the computational grid adaptation each time the shape of the controlled boundary changes) are considered as extra state equations, next to the fluid flow

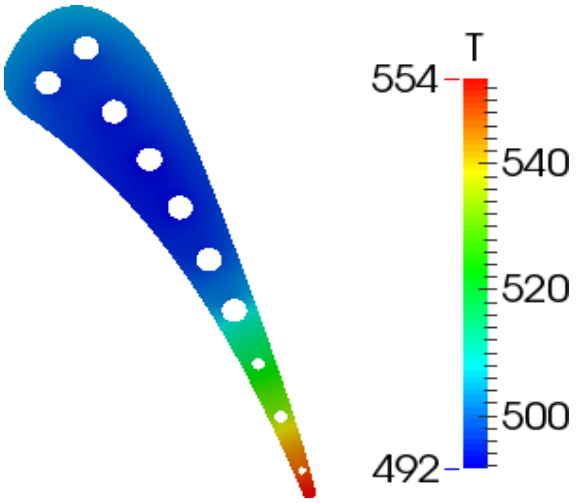

(a) T^S on the initial geometry

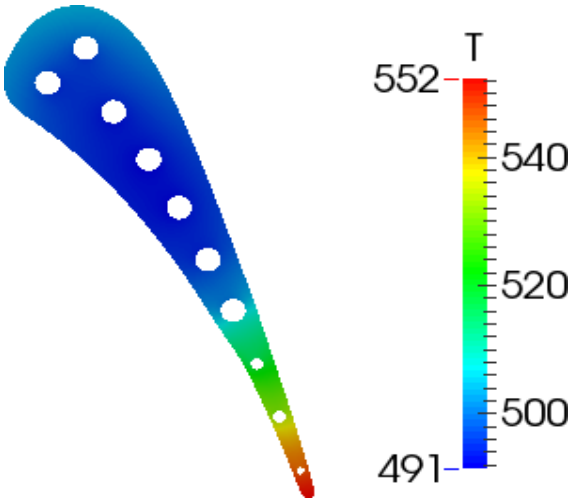

(b) T^S on the optimal geometry

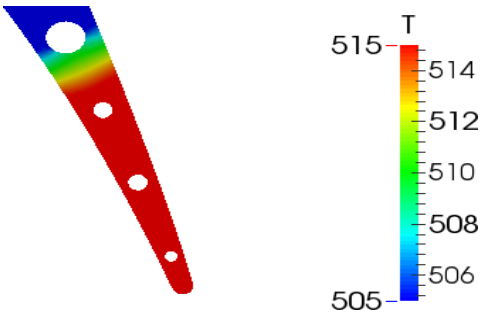

(c) Initial span $T_{crit} - T_{safe}$.

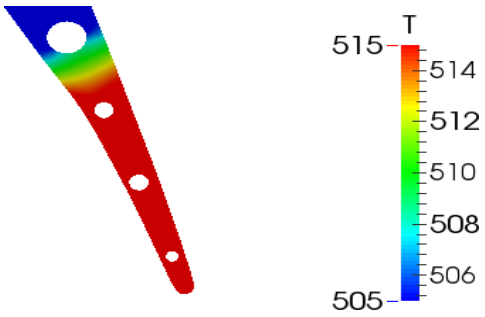

(d) Final span $T_{crit} - T_{safe}$.

Figure 2: Turbulent flow around the 2D blade of a turbine stator. Minimization of J_{maxT}. Temperature over the initial and optimized blade.

PDEs and the PDEs governing heat conduction over the solid domain. By including them into the augmented objective function, an extra set of adjoint grid displacement PDEs results which must be solved, since it contributes to the gradient formula. This method, which is in fact an extension of a similar technique recently proposed by the same group for shape optimization problems in fluid mechanics only, is referred to as the Enhanced-Surface Integral (E-SI) adjoint approach. Among other, we demonstrated that this is as accurate as the more expensive adjoint method which includes field integrals depending on the grid sensitivities and as fast as the most frequently used adjoint formulation with gradients which depend only on surface/boundary integrals; the latter is demonstrated to compute quite wrong derivatives due to the assumptions made during its development.

Acknowledgement:
The early phase of this development was funded by Volkswagen AG (Group Research, K-EFFG/V, Wolfsburg, Germany). The authors would like to thank Dr. C. Othmer for

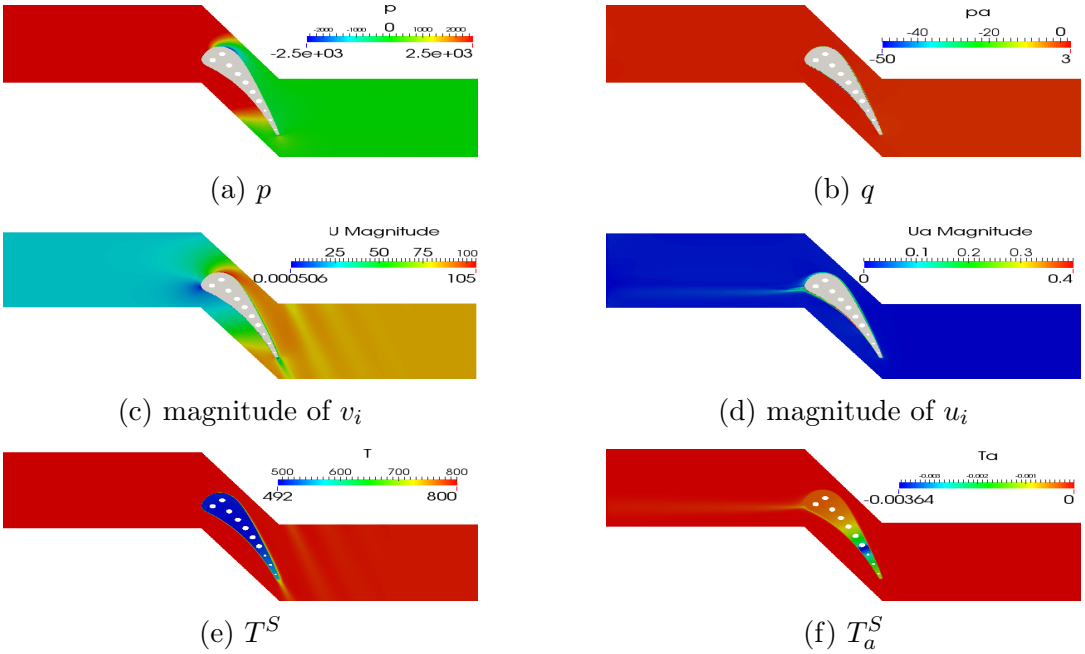

(a) p (b) q

(c) magnitude of v_i (d) magnitude of u_i

(e) T^S (f) T_a^S

Figure 3: Turbulent flow around the 2D blade of a turbine stator. Minimization of J_{maxT}. Primal and adjoint fields over Ω_F and Ω_S for the initial geometry.

his support.

REFERENCES

[1] W.K. Anderson and V. Venkatakrishnan. Aerodynamic design optimization on unstructured grids with a continuous adjoint formulation. *Computers & Fluids*, 28(4-5):443–480, 1999.

[2] B.H. Dennis, I.N. Egorov, G.S. Dulikravich, S. Yoshimura. Optimization of a large number of coolant passages located close to the surface of a turbine blade. In *Proceedings of ASME Turbo Expo 2003 – Power for Land, Sea, and Air*, Atlanta, Georgia, 16 - 19 June 2003.

[3] H. Narten, C. Correia, C. Othmer, R. Radespiel. Adjoint-based cooling efficiency optimization of turbulent ducted flows. In P. Nithiarasu N. Massarotti and B. Sarler, editors, *Third International Conference on Computational Methods for Thermal Problems, THERMACOMP2014*, pages 134–137, Lake Bled, Slovenia, June 2-4 2014.

[4] A. Jameson. Aerodynamic design via control theory. *Journal of Scientific Computing*, 3:233–260, 1988.

[5] A. Jameson and S. Kim. Reduction of the adjoint gradient formula in the continuous limit. In *AIAA Paper 2003-0040, 41th Aerospace Sciences Meeting and Exhibit*, Reno, Nevada, January 2003.

[6] I.S. Kavvadias, E.M. Papoutsis-Kiachagias, G. Dimitrakopoulos, and K.C. Giannakoglou. The continuous adjoint approach to the k–ω SST turbulence model with applications in shape optimization. *Engineering Optimization*, 47(11):1523–1542, 2015.

[7] I.S. Kavvadias, E.M. Papoutsis-Kiachagias, and K.C. Giannakoglou. On the proper treatment of grid sensitivities in continuous adjoint methods for shape optimization. *Journal of Computational Physics*, 301:1–18, 2015.

[8] K.C. Giannakoglou, E.M. Papoutsis-Kiachagias, I.S. Kavvadias, K.T. Gkaragkounis. Continuous Adjoint in Shape & Topology Optimization - Recent Developments & Applications. In *Seminar on Adjoint CFD Methods in Industry and Research*, pages 43–52, Wiesbaden, Germany, 24 - 25 November 2016.

[9] K.C. Kiani M. Zeinalpour, K. Mazaheri. A coupled adjoint formulation for non-cooled and internally cooled turbine blade optimization. *Applied Thermal Engineering*, 105:327–335, 2016.

[10] D.I. Papadimitriou and K.C. Giannakoglou. A continuous adjoint method with objective function derivatives based on boundary integrals for inviscid and viscous flows. *Journal of Computers & Fluids*, 36(2):325–341, 2007.

[11] P. Spalart and S. Allmaras. A one-equation turbulence model for aerodynamic flows. In *AIAA Paper 1992-0439, 30th Aerospace Sciences Meeting and Exhibit*, Reno, Nevada, 6-9 January 1992.

[12] A.S. Zymaris, D.I. Papadimitriou, K.C. Giannakoglou, and C. Othmer. Continuous adjoint approach to the Spalart-Allmaras turbulence model for incompressible flows. *Computers & Fluids*, 38(8):1528–1538, 2009.